IEEE Access
Multidisciplinary | Rapid Review | Open Access Journal

Received September 2, 2017, accepted September 26, 2017, date of publication September 29, 2017, date of current version November 7, 2017.

Digital Object Identifier 10.1109/ACCESS.2017.2757947

Wireless Energy Harvesting by Direct Voltage Multiplication on Lateral Waves From a Suspended Dielectric Layer

LOUIS WY LIU[1], QINGFENG ZHANG[1], YIFAN CHEN[2], MOHAMMED A. TEETI[1], AND RANJAN DAS[1,3]

[1]Electrical and Electronics Engineering Department, Southern University of Science and Technology, Shenzhen 154108, China
[2]School of Engineering, University of Waikato, Hamilton 3240, New Zealand
[3]School of Engineering, IIT Bombay, Mumbai 400076, India

Corresponding author: Qingfeng Zhang (zhangqf@sustc.edu.cn)

This work was supported in part by the Guangdong Natural Science Funds for Distinguished Young Scholar under Grant 2015A030306032, in part by the Guangdong Special Support Program under Grant 2016TQ03X839, in part by the National Natural Science Foundation of China under Grant 61401191, in part by the Shenzhen Science and Technology Innovation Committee funds under Grant KQJSCX20160226193445, Grant JCYJ20150331101823678, Grant KQCX2015033110182368, Grant JCYJ20160301113918121, Grant JSGG20160427105120572, and in part by the Shenzhen Development and Reform Commission Funds under Grant [2015] 944.

ABSTRACT This paper explores the feasibility of wireless energy harvesting by direct voltage multiplication on lateral waves. Whilst free space is undoubtedly a known medium for wireless energy harvesting, space waves are too attenuated to support realistic transmission of wireless energy. A layer of thin stratified dielectric material suspended in mid-air can form a substantially less attenuated pathway, which efficiently supports propagation of wireless energy in the form of lateral waves. The conductivity of the suspended dielectric layer does not appear to be a critical factor rendering propagation of lateral waves impossible. In this paper, a mathematical model has been developed to simulate wireless energy harvesting over a suspended layer of stratified dielectric material. The model has been experimentally verified with the help of a novel open-ended voltage multiplier designed to harvest energy from ambient electromagnetic fields.

INDEX TERMS Energy harvesting, stratified ground, Goubau line, Avremenko diode configurations, trapped surface waves, transverse magnetic modes, TM modes, TEM modes, Zenneck Waves, lateral waves, ground waves.

I. INTRODUCTION

Whilst many researchers of this date are still struggling to transmit wireless energy over just a few meters by magnetic coupling, the feasibility of long range wireless energy harvesting has long been proven beyond any doubt by Marconi [1]–[3]. In one of Marconi's early experiments, wireless energy was successfully and safely transmitted and harvested over 2 miles of a hilly area by grounding and lengthening monopole antenna as a way to reduce the aperture size of the antenna. Marconi concluded from his first breakthrough experiment that his antenna radiated vertically polarized radio waves that could travel distances much longer than other conventional counterparts. Later, he even achieved non-line-of-sight (NLOS) propagation of wireless power across the Atlantic Ocean [4]–[7].

Throughout the last century, there have been many unsuccessful attempts to use Zenneck's version of surface waves to explain Marconi's work [8]–[12]. The absence of an appropriate theory for surface waves or their derivatives does not necessarily mean that Marconi's achievement in long range wireless power transfer (WPT) has to be erased from history. Towards the end of the last century, Wait came forwards with a concept of trapped surface waves in a stratified ground [13]. Trapped surface wave is an evanescent wave propagating by successive internal reflections due to an incident electromagnetic wave striking at an interface with an angle greater than the critical angle. However, the energy from trapped surface waves has not been found to be significant in many situations [14]. In the same decade, another much more promising concept known as *lateral wave* was used by King to explain the dominant electromagnetic waves propagating over the

surface of a stratified ground [15]. This lateral wave is a vertically polarized electromagnetic wave on the top surface of the ground as a result of an incident electromagnetic wave striking the air-ground interface from below at exactly the critical angle [16], [17]. For an interface between two different dielectric media, the critical angle is only applicable to the dielectric medium with a higher refractive index. To excite this lateral wave, it is logical to bury the lower end of transmitting and receiving aerials into the dielectric layer with a higher refractive index in much the same way as grounding a monopole antenna in Tesla's or Marconi's work [2], [16]–[18]. In fact, the vertically polarized radio wave as referred by Marconi or ground current referred by Nikola Tesla is most likely equivalent to the lateral wave referred by King, Tamir and many other researchers in the field of wireless energy harvesting.

Ironically, most of the recently published systems for WPT are still based on space waves, including the magnetic coupled waves for near field applications and the Hertzian radio waves for far field applications. Space waves are known to be inefficient because a significant amount of energy in an unguided space wave is lost by radiation. On the other hand, transmitting a large electric power through free space will directly impose interference to the present communication systems. Another little-known fact is that an extremely low-frequency space waves can potentially trigger release of toxins from microvesicles of monocytic leukaemia cells [19]. The authors believe that delivering electric power through the physical ground, ocean or the wall of a building is a far more logical solution.

In this article, the feasibility of wireless energy harvesting by voltage multiplication on lateral waves is explored by an unconventional means. Instead of transmitting a wireless energy through a thick layer of a concrete ground, we extend the original idea of Tesla's or Marconi's to harvest a wireless energy from a thin layer of dielectric material suspended in mid-air. We begin our presentation by formulating a mathematical model of electromagnetic waves associated with a dielectric layer suspended in mid-air. The theoretical work will be substantiated with the results of WPT experiments based on a little known open-ended voltage multiplier.

Applications of lateral-wave-based WPT will be explored in areas of wireless communication according to the well understood differences between surface waves and space waves as summarized in Table 1.

TABLE 1. Differences between space waves and surface waves.

	Space Waves	Surface Waves
Examples	Magnetically coupled waves, radio waves, light waves, thermal radiation, X ray, visible light, microwave, infrared, gamma rays etc.	Lateral waves, trapped surface waves, chiral surface waves, surface-wave-sustained plasma, surface plasmon polariton, over-dense plasma, etc.
Basic Features	Traveling at the speed of light with energy lost by radiation into free space.	Traveling at below the speed of light without any radiation.
Harvesting and Rectification	A wide aperture antenna is needed to capture the space waves, which is usually impedance matched to 50Ω from 377Ω and rectified into a twin-wire DC power.	The surface power can be harvested by any single refractive or conductive medium and directly rectified into a DC without down-converting the transmission line impedance.
Harvested Output	1) Current density is relatively low and spread everywhere in free space.	1) Current density is relatively high and concentrated along the interface between two different dielectrics.
	2) The harvested power is typically inversely proportional to the square of distance from the source, i.e., an inverse-square law.	2) The harvested power is inversely proportional to the transmission distance
Guided or Unguided	Unguided	Guided in the form of Transverse Magnetic Modes or Transverse Electric Modes
Safety	Contributes to health risks [19][34-36] and increases interference in existing wireless networks.	Relatively safe due to the slower phase velocity and hence the shorter wavelength for a fixed frequency [34-36].
Propagation modes	Traveling in a straight line only.	Being bound to or following the contour a curved interface between two dielectric materials.

II. ELECTROMAGNETIC MODELING OF A SUSPENDED LAYER OF A DIELECTRIC MATERIAL

While stratified ground with a perfect conducting bottom plane as a medium for transmission of trapped surface waves and lateral waves has been extensively studied [13]–[15], [20], the results of our investigation reveal that a suspended layer of dielectric material can be modeled as a 4-layered stratified ground with imperfectly conducting ground. The stratified ground with imperfectly conducting ground can support propagation of both trapped surface waves and lateral waves. The existence of trapped surface waves is possible if and only if the suspended layer of dielectric material is sufficiently thick, perhaps, thicker than half of the wavelength. To rule out the possibility of trapped surface waves being present to a significant extent, we have chosen to study the suspended dielectric layer with a thickness substantially smaller than half of the wavelength. Examples of this stratified ground with imperfectly conducting bottom plane include a table top, an iron-reinforced concrete wall or any suspended dielectric layer coated with an oxide.

Fig. 1 illustrates how a suspended dielectric layer can be visualized as a conventional four-layered stratified ground

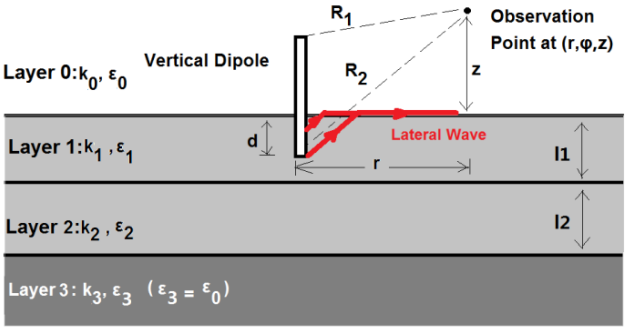

FIGURE 1. Configuration of wireless power transfer involving a dipole vertically mounted on the surface of a suspended dielectric layer.

with imperfect conducting plane at the bottom. This dielectric configuration is similar to the 4-layered ground that has already been considered in other studies [14], [20], with an exception that the bottom layer in the present work is a layer of air with an extremely small conductivity. The relative permittivities of layers 0, 1, 2 and 3 are respectively ε_0, ε_1, ε_2 and ε_3, where $\varepsilon_0 = \varepsilon_3 = 1$. The thicknesses of layer 0 and layer 3 is assumed to be infinity. The distance between the transmitting antenna and the receiving antenna is denoted by r. Layer 1 and layer 2, respectively, have a finite thickness l_1 and l_2. The length of the vertically mounted dipole is of approximately 1/4 -wavelength of the chosen operating frequency. The apparent pathway of a lateral wave is highlighted in red. As shown in Fig. 1, the deeper the dipole is submerged underneath the top surface of layer 1, the more energy radiated out from the base of the vertical dipole will be striking the interface between air and layer 1 at critical angle and the more energy will be converted into a lateral wave.

In Fig. 1, the wave numbers in all the layers are:

$$k_0 = k_3 = \omega\sqrt{\mu_0\varepsilon_0} \tag{1a}$$

$$k_j = \omega\sqrt{\mu\left(\varepsilon_0\varepsilon_{rj} + i\left(\frac{\sigma_j}{\omega}\right)\right)}, \quad \text{with } j = 1, 2 \tag{1b}$$

where ω is the angular frequencies in radian, μ and μ_0 are respectively the permeabilities of layer j and free space and σ_j is the conductivity of layer j.

Using modal analysis, the time-varying transverse magnetic field in the multi-layered ground can be modeled in frequency domain and can be expressed as in (2) [14], [20]. The formula given in (2) as follows is applicable to both the transmitting and receiving antennas.

$$\begin{aligned} B_\phi(\rho, z) = {} & \frac{i\mu_0}{4\pi}\int_0^\infty \left[\exp(i\gamma_0|z-d|)\right]\gamma_0^{-1}J_1(\lambda r)\,\lambda^2 d\lambda \\ & + \frac{i\mu_0}{4\pi}\int_0^\infty \left[\exp(i\gamma_0(z+d))\right]\gamma_0^{-1}J_1(\lambda r)\,\lambda^2 d\lambda \\ & + \frac{i\mu_0}{4\pi}\int_0^\infty \left[-(Q+1)\exp(i\gamma_0(z+d))\right]\gamma_0^{-1} \\ & \times J_1(\lambda r)\,\lambda^2 d\lambda, \end{aligned} \tag{2}$$

where λ is the wavelength, $J_1(\ldots)$ is the Bessel function of the first kind of order 1 and γ_j is the propagation constant at layer j defined as

$$\gamma_j = \sqrt{k_j^2 - \lambda^2}, \tag{3}$$

Q, which is the reflection coefficient of the half-space due to the multi-layered configuration, can be expressed as:

$$Q = -\frac{\gamma_0 - \frac{k_0^2}{\omega\mu_0}Z_s}{\gamma_0 + \frac{k_0^2}{\omega\mu_0}Z_s}, \tag{4}$$

In (4), Z_s represents the surface impedance for the 4-layered stratified ground configuration as defined in [15]:

$$Z_s = \frac{\left[\begin{array}{l}\gamma_1\mu_0\omega k_1^2\left(\gamma_2^2k_3^2\tan(\gamma_2 l_2)\,i - \gamma_2\gamma_3k_2^2\right) \\ +\gamma_1\mu_0\omega\left(\begin{array}{l}\gamma_1\gamma_3k_2^4\tan(\gamma_1 l_1)\tan(\gamma_2 l_2) \\ +i\gamma_1\gamma_2k_2^2k_3^2\tan(\gamma_1 l_1)\end{array}\right)\end{array}\right]}{k_1^2\left[\begin{array}{l}i\gamma_1\gamma_3k_2^4\tan(\gamma_2 l_2) - \gamma_1\gamma_2k_2^2k_3^2 \\ +\gamma_2^2k_1^2k_3^3\tan(\gamma_1 l_1)\tan(\gamma_2 l_2) \\ +i\gamma_2\gamma_3k_1^2k_2^2\tan(\gamma_1 l_1)\end{array}\right]}. \tag{5}$$

The first and second integral terms on the right side of (2) represents the direct space wave and the reflected space wave respectively. These two integral terms have been evaluated by King *et al.* [15]:

$$\begin{aligned} & \frac{i\mu_0}{4\pi}\int_0^\infty \left[\exp(i\gamma_0|z-d|)\right]\gamma_0^{-1}J_1(\lambda r)\,\lambda^2 d\lambda \\ & \qquad = -\frac{i\mu_0}{4\pi}\exp(ik_0R_1)\left(\frac{\rho}{R_1}\right)\left(\frac{ik_0}{R_1} - \frac{1}{R_1^2}\right), \end{aligned} \tag{6a}$$

$$\begin{aligned} & \frac{i\mu_0}{4\pi}\int_0^\infty \left[\exp(i\gamma_0(z+d))\right]\gamma_0^{-1}J_1(\lambda r)\,\lambda^2 d\lambda \\ & \qquad = -\frac{i\mu_0}{4\pi}\exp(ik_0R_2)\left(\frac{r}{R_2}\right)\left(\frac{ik_0}{R_2} - \frac{1}{R_2^2}\right). \end{aligned} \tag{6b}$$

The third integral term represents a superimposition of the trapped surface wave and the lateral wave. This integral term is complex and it has to be resolved by Cauchy Riemann's residue theorem. To begin with, Z_s in (5) is then substituted into (4). The quantity $(Q+1)$ in the third integral of (2) is then symbolically derived into the form of a rational expression, using MATLAB or a similar mathematical analysis tool:

$$(Q+1) = 2ik_0^2\gamma_1\frac{A(\lambda)}{q(\lambda)}, \tag{7}$$

where the nominator $A(\lambda)$ is given by:

$$\begin{aligned} A(\lambda) = {} & -i\tan(\gamma_2 l_2)\left[\gamma_2^2k_3^2k_1^2 - i\gamma_1\gamma_3k_2^4\tan(\gamma_1 l_1)\right] \\ & + \gamma_2k_2^2\left[\gamma_3k_1^2i + \gamma_1k_3^2\tan(\gamma_1 l_1)\right], \end{aligned} \tag{8a}$$

and the denominator $q(\lambda)$ is:

$$\begin{aligned} & q(\lambda) \\ & = \tan(\gamma_2 l_2)\left[\begin{array}{l}\gamma_0\gamma_1\gamma_3k_1^2k_2^4i + \gamma_0\gamma_2^2k_1^4k_3^2\tan(\gamma_1 l_1) \\ +\gamma_1^2\gamma_3k_0^2k_2^4\tan(\gamma_1 l_1)\,i + \gamma_1\gamma_2^2\gamma_0^2k_1^2k_3^2i\end{array}\right] \\ & \quad + \gamma_2k_2^2\left[\begin{array}{l}\gamma_1^2k_0^2k_3^2\tan(\gamma_1 l_1)\,i + \gamma_0\gamma_3k_1^4\tan(\gamma_1 l_1)\,i \\ -\gamma_0\gamma_1k_3^2k_1^2 - \gamma_1\gamma_3k_0^2k_1^2\end{array}\right]. \end{aligned} \tag{8b}$$

When a dielectric layer is suspended in mid-air, we have $k_3 = k_0$. Thus. (8a) and (8b) can be simplified as:

$$A(\lambda) = \gamma_2 k_1^2 \left(\gamma_2 k_0^2 \tan(\gamma_2 l_2) + \gamma_1 k_2^2 i\right) - \gamma_1 k_2^2 \tan(\gamma_1 l_1)\left(\gamma_2 k_0^2 - i k_2^2 \gamma_0 \tan(\gamma_2 l_2)\right), \quad (9a)$$

$$q(\lambda) = \tan(\gamma_2 l_2)\begin{bmatrix}\gamma_0^2\gamma_1 k_1^2 k_2^4 i + \gamma_0\gamma_1^2 k_2^4 k_0^2 \tan(\gamma_1 l_1) \\ \gamma_2^2\gamma_0 k_0^2 k_1^4 \tan(\gamma_1 l_1)\, i + \gamma_1\gamma_2^2 k_0^4 k_1^2 i\end{bmatrix} + \gamma_2 k_2^2 \begin{bmatrix}\gamma_0^2 k_1^4 \tan(\gamma_1 l_1)\, i + k_0^4\gamma_1^2 \tan(\gamma_1 l_1)\, i \\ -2\gamma_0\gamma_1 k_0^2 k_1^2\end{bmatrix}. \quad (9b)$$

Using the relationship between Bessel function and the Hankel function, the third term of (2) can be rewritten as follows:

$$\frac{i\mu_0}{4\pi}\int_0^\infty \left[-(Q+1)\exp(i\gamma_0(z+d))\right]\gamma_0^{-1} J_1(\lambda r)\lambda^2 d\lambda = \frac{i\mu_0 k_0}{4\pi}\int_{-\infty}^\infty \left[\frac{A(\lambda)}{q(\lambda)}\exp(i\gamma_0(z+d))\right]\gamma_0^{-1} H_1^{(1)}(\lambda r)\lambda^2 d\lambda \quad (10)$$

where $H_1^{(1)}(\ldots)$ is the first order Hankel function of first kind. By Cauchy-Riemann's residue theorem, (10) can be further expressed as (11), as shown at the bottom of this page, for $j = 0, 1, 2, ..$

III. LATERAL WAVES IN A SUSPENDED LAYER OF LOSSY DIELECTRIC

The first summation term on the right side of (11) refers to the trapped surface wave due to the poles of the integrand in (10), λ_k. The poles can be numerically resolved by equating $q(\lambda)$ in (8b) to zero. As has been pointed by Li [20], (11) will yield *n+1* poles between k_i and k_{i+1} if the electrical properties of the multi-layered ground configuration satisfy the following inequality relationship:

$$n\pi \le l_i\sqrt{k_i^2 - k_0} \le (n+1)\pi s. \quad (12)$$

To support propagation of trapped surface waves, a dielectric layer should have a thickness at least half wavelength. The integrand in (10) can be without any pole if the suspended dielectric layer is too thin. This means that there will not be any significant contribution of energy to the receiving end due to a trapped surface wave if the suspended dielectric layer is too thin. However, the upper and lower interfaces of the dielectric layer remain reflective even in the absence of any trapped surface waves. If an incoming electromagnetic wave strikes at either interface of an extremely thin dielectric layer at critical angle, the electromagnetic energy will be forced to propagate along the upper and lower interface in the form of a lateral wave with an extremely high current density.

Mathematically, this lateral wave can be derived by evaluating the last summation term of (11), which is due to the integral contribution of all the branch cuts in the complex plane. The contribution of the integral term along the branch cuts at k_1 is essentially zero. Layer 3 can be regarded as an imperfectly conducting layer. Since the lateral wave from the interface between layer 3 and layer 2 has to propagate through a much longer and more attenuated pathway before reaching the receiver, the contribution of the branch cut k_3 to the receiving end can be assumed to be negligible although this assumption can be invalid if the suspended dielectric layer is too thin. The main contribution to the lateral wave is due to the branch cut at k_0. This integral term needs to be resolved using Fresnel integral and a complementary error-function. The approach proposed in [20] is adopted. To start with, the following approximation is made:

$$\lambda = k_0(1 + i\tau) \quad (13a)$$

$$H_1^{(1)}(\lambda r) \approx \sqrt{\frac{2}{\pi k_0 r}}\exp\left(i\left(k_0 r - \frac{3\pi}{4}\right)\right)\exp\left(-k_0 r\tau^2\right) \quad (13b)$$

$$\gamma_j \approx \gamma_{j0} = \sqrt{k_j^2 - k_0^2}, \quad \text{for } j = 1, 2 \quad (13c)$$

Finally, the expressions in (13a), (13c) and (13b) are substituted into the large integral term of (11) to obtain the following expression for the lateral wave:

$$\frac{-i\mu_0 k_0^2}{4\pi}\left\{\sum_j \int_\Gamma \frac{A(\lambda)\gamma_1 \exp(i\gamma_0(z+d))\, H_1^{(1)}(\lambda r)\lambda^2}{q(\lambda)\gamma_0} d\lambda\right\} \approx \frac{-\mu_0 k_0^3}{2}\sqrt{\frac{1}{\pi k_0 r}}\exp(ik_0 R_2 - ip)F(p)\frac{ik_0^2\gamma_1 A(k_0)}{\gamma_0 \frac{dq(\lambda)}{d\lambda}\Big|_{\lambda=k_0}} \quad (14)$$

$$-\frac{i\mu_0 k_0}{4\pi}\sum_k \int_{\angle k}\left[\frac{A(\lambda)}{q(\lambda)}\exp(i\gamma_0(z+d))\right]\gamma_0^{-1} H_1^{(1)}(\lambda r)\lambda^2 d\lambda = \frac{-i\mu_0 k_0^2}{4\pi}\left\{\begin{array}{l} 2\pi i\sum_k \dfrac{A(\lambda_k)\exp\left(i(z+d)\sqrt{k_0^2-\lambda_k^2}\right)\lambda_k^2\sqrt{k_1^2-\lambda_k^2}H_1^{(1)}(\lambda_k r)}{\frac{dq(\lambda)}{d\lambda}\Big|_{\lambda=\lambda_k}\sqrt{k_0^2-\lambda_k^2}} \\ +\sum_j \int_{\Gamma_j} \dfrac{A(\lambda)\gamma_1\exp(i\gamma_0(z+d))\, H_1^{(1)}(\lambda r)\lambda^2}{q(\lambda)\gamma_0} d\lambda \end{array}\right\} \quad (11)$$

$$\frac{A\left(k_0\right)}{\gamma_0 \frac{dq(\lambda)}{d\lambda}\Big|_{\lambda=k_0}} = \frac{\left[\begin{array}{l}\gamma_{20}k_1^2\left(\gamma_{30}k_2^2 i+\gamma_{20}k_3^2\tan\left(\gamma_{20}l_2\right)\right)\\ +\gamma_{10}k_2^2\tan\left(\gamma_{10}l_2\right)\left(\gamma_{20}k_3^2-i\gamma_{30}k_2^2\tan\left(\gamma_{20}l_2\right)\right)\end{array}\right]}{\left[\begin{array}{l}-k_0k_1^4\tan\left(\gamma_{10}l_1\right)\left(-k_0^2k_3^2\tan\left(\gamma_{10}l_2\right)+k_2^2k_3^2\tan\left(\gamma_{20}l_2\right)+i\gamma_{20}\gamma_{30}k_2^2\right)\\ +\gamma_{10}k_0k_1^2k_2^2\left(\gamma_{20}k_3^2-i\gamma_{30}k_2^2\tan\left(\gamma_{20}l_{20}\right)\right)\end{array}\right]} \tag{15a}$$

(15a), as shown at the top of this page, defines the last fraction of (14). In equation (14), $F(p)$ is the Fresnel integral:

$$F\left(p\right)=\frac{1}{2}\left(1+i\right)-\int_0^p \frac{\exp\left(it\right)}{\sqrt{2\pi t}}dt \tag{15b}$$

with

$$p=\frac{k_0 r}{2}\left[\frac{z+d}{r}+\frac{ik_0^2\gamma_1 A\left(k_0\right)}{\frac{dq(\lambda)}{d\lambda}\Big|_{\lambda=k_0}}\right]^2 \tag{15c}$$

IV. HARVESTING ENERGY FROM LATERAL WAVES BY DIRECT VOLTAGE MULTIPLICATION

In one of Tesla's lectures [18], Tesla has highlighted the fact that power transmission by one-wire transmission line is equivalent to wireless power transfer. Although the link between power transfer by one wire and wireless power transmission has not been well explored in other research literature, it was found in a recently published work [21] that the energy from a time-varying electromagnetic field can be captured by a one wire transmission without any antenna. In this work, wireless energy is harvested from lateral waves on the surface of a suspended dielectric layer using a little known open-ended voltage multiplier. Fig. 1 illustrates the schematic diagram of the open-ended voltage multiplier similar to the one proposed in [21]. This open-ended voltage multiplier has an input terminated by an open-circuited Goubau line. Goubau line is one-wire transmission line having characteristic impedance very close to the characteristic impedance of free space. If the end of the Goubau is left open-circuited, it becomes a monopole antenna which captures ambient electromagnetic field right on the top surface of the suspended dielectric layer without any other form of antenna.

The voltage sensed by the Goubau line is rectified into a DC voltage using the well-known Avremenko's diode configuration formed by diodes *D1* and *D2* [22], [23]. The voltages across *D1* and *D2* are very limited because each of the diodes has its own maximum forward voltage. However, before reaching the output, the voltages across *D1* and *D2* can undergo voltage multiplication by the differential voltage multiplier formed by diodes *D3*, *D4*, *D5* and capacitances C_1, C_2, C_3 and C_4.

The output voltage is the sum of the voltages of all the diodes *D1-D6*. The fundamental AC voltage across *D1* and *D2*, $2V_D$, depends on the time-varying electromagnetic field captured by the Goubau line, which cannot be changed by changing the circuit topology. However, the AC voltage across each of all other diodes *D3-D6* can be force-increased to a maximum of $2V_D$ by introducing the AC shorts formed by capacitors C_1-C_4. All the diodes used in this circuit are assumed to be the same and all the discrete capacitors used in the circuit are assumed to have a capacitance C. If the parasitic inductance L_p is sufficiently small, then the output voltage can be derived and approximated using the approach given in Appendix I into the following [21]:

$$V_{out}=10V_D-\frac{nKT}{q}\ln\left[\frac{4\pi qV_D}{nKT}\right]+\frac{2nKT}{q}\ln\left[\frac{qI_S}{nCfnKT}\right] \tag{16}$$

where n is the intrinsic ideality of the diode. I_s is the reverse saturation current of each of the diodes. nKT/q is the threshold voltage, which is typical *25 mV* at room temperature. f is the operating frequency. The formula given in (16) assumes that the load resistance is infinitely large. The last term of (16) also accounts for the frequency dependent effects due to the capacitances in the layout.

The prototypes for the proposed open-ended voltage multiplier have been fabricated on a Rogers Duroid (TM) substrate 4350B with thickness=1.52mm. Fig. 2 shows the details of the proposed open-ended voltage multiplier. The diodes used for fabricating prototypes in this work were SMS7630-093 from Skyworks. The schematic diagram, the photo of the fabricated prototype and the simulated electric field distribution at 1.24 GHz are respectively shown in Figs. 2a, 2b and 2c.

The input impedance of the opened voltage multiplier was approximately 400 ohm according to electromagnetic simulation. It should be noted that, for the purpose of verifying the design against the simulation, the output voltages of the proposed voltage multipliers were first measured as a function of frequency when the input terminals were fed with a 50 ohm microwave power source (E8267D, Agilent Technologies) at 20 dBm. The measured results together with the results of layout/schematic co-simulation done using Keysight's Momentum are shown in Fig. 2d.

V. SIMULATED AND MEASURED RESULTS OF BASIC WPT CONFIGURATION

The feasibility of wireless power transfer based on the proposed voltage multipliers has been explored using the experimental configurations as shown in Figs 3a and 3b. Fig 3a illustrates an experimental configuration where the transmitted energy is expected to be primarily a lateral wave. Fig 3b shows an experimental configuration focusing on space waves only. In either configuration, the transmitting end is mounted with a base-fed monopole antenna formed by a planar Goubau line, and the receiving end is vertically

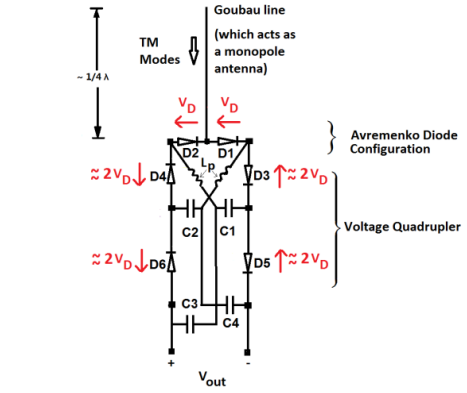

(a)

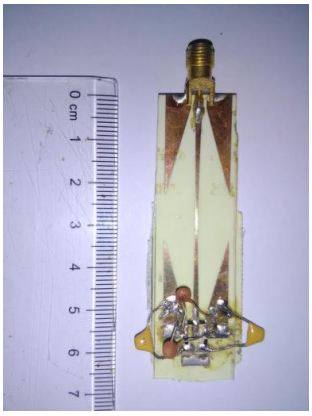

(b)

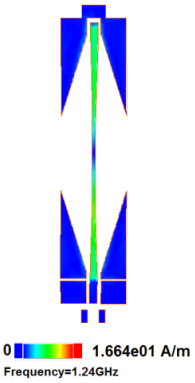

(c)

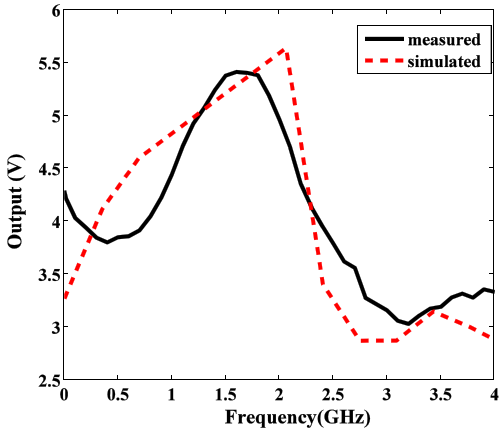

(d)

FIGURE 2. The proposed open-ended voltage multiplier loaded with a 450 ohm resistor: a) the schematic diagram; b) the fabricated circuit. c) Electric field distribution simulated on the layout using Keysight's Momentum. d) Output voltage as a function of frequency when the input is terminated with 50 ohm instead of being left open-circuited.

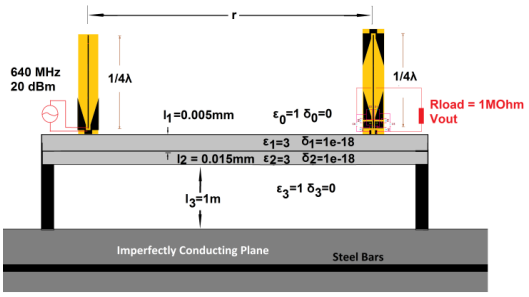

(a)

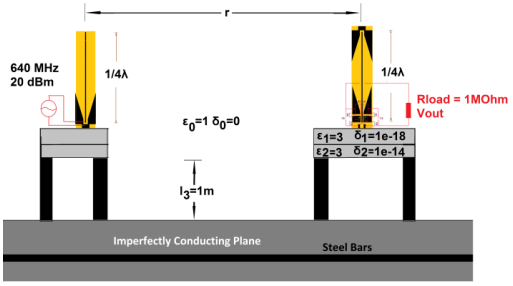

(b)

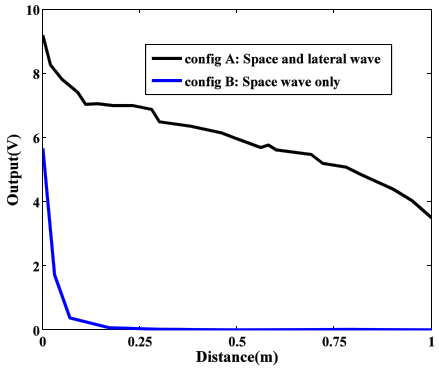

(c)

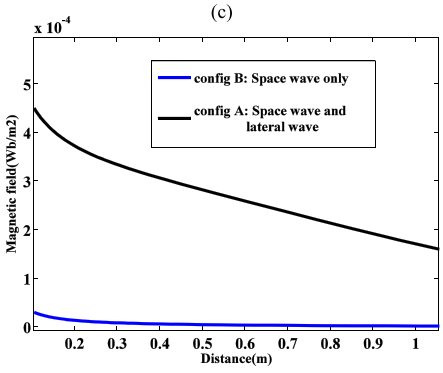

(d)

FIGURE 3. Experiments on wireless energy harvesting at 640 MHz: a) Configuration A: with lateral waves and space waves involved. b) Configuration B: with space waves involved only. c) Measured output voltage as a function of distance for configurations A and B; d) Simulated magnetic field at the receiving end as a function of distance configurations A and B.

mounted with the proposed open-ended voltage multiplier terminated with a *1 MΩ* load resistor. The measured results of this work are shown in Fig. 3c.

In addition to the above measurement, the experimental configurations as shown in Figs. 3a and 3b have been modeled according to (1)-(15). The model, which has been coded in

MATLAB ™, has been used to simulate these experiments. The simulation results are shown in Fig. 3d.

The table top was a layer of dry wood covered with a thin layer of plastic coating. The relative permittivity and the conductivity of dry wood are respectively 2.1 and 1e-14 S/m. The relative permittivity and the conductivity of the plastic cover are respectively 3 and 1e-16 S/m. The legs of the table are made with steel. The table top is 1m away from the ground, which is another imperfectly conducting plane. The ground is made with steel-reinforced concrete. The dielectric constant of concrete is known to be approximately 5. However, because of the presence of steel bars in the concrete floor and steel legs of the table, the equivalent conductivity of the air underneath the table should not be assumed to be zero. For the purpose of analysis, an equivalent conductivity of air underneath the table top has been estimated by experiment. By measurement at different frequencies, we have estimated that the equivalent conductivity of air underneath the table top is about 1e-18 S/m.

The model given by (1-16) has been coded in MATLAB ™. The parameters used to simulate the magnetic component of the lateral wave are:

$$\varepsilon_0 = 8.85e-12, \quad \mu_0 = 4\pi e-7, \; f = 640MHz,$$

$$\varepsilon_1 = 2.8, \quad \sigma_1 = 1e-16, \; \varepsilon_2 = 2.1,$$

$$\sigma_2 = 1e-14, \quad \varepsilon_3 = 1, \; \sigma_3 = 1e-18,$$

$$l_1 = 0.0005m, \quad l_2 = 0.015m.$$

It can be observed from Figs 3c and 3d that the harvested energy at the receiving end is much higher in the presence of a lateral wave. In this work, the amplitude of the magnetic field due to the trapped surface wave was too small to be plotted.

VI. CASCADING OPEN-ENDED VOLTAGE MULTIPLIERS IN SERIES

Whilst the energy that can be harvested at a single observation point is highly limited, the results of our investigation reveal that multiple pieces of the proposed open-ended voltage multiplier can be connected in series to boost the overall efficiency. This means that we can have a number of serially connected open-ended voltage multipliers spanning an area to take advantage of every antinode of a lateral wave.

It was found from another experiment as shown in Fig. 4 that the total output voltage was maximized when each two neighboring pieces of the open-ended voltage multiplier are spaced at exactly half of the free-space wavelength apart. In this experimental configuration, the source at the transmitting end was powered at 20dBm, 1.24 GHz. At the receiving end, two identical open-ended voltage multipliers connected in series were spaced at two different distances: 5cm and 10 cm, corresponding to 1/4 λ and 1/2 λ. The measured results were curved fit and shown in Fig. 4b. It can be observed that the output voltage becomes higher at all frequencies if two open-ended voltage multipliers cascaded series are spaced at 1/2 λ.

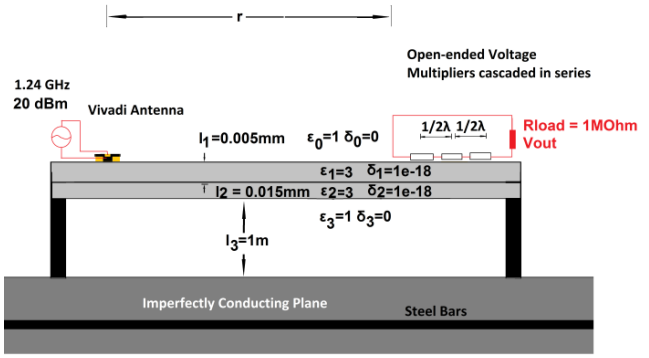

(a)

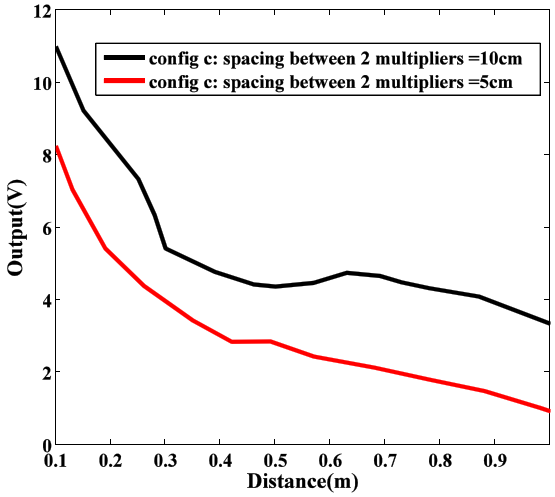

(b)

FIGURE 4. Configuration C: Cascading open-ended voltage multipliers for wireless energy harvesting. a) Experimental configuration; and b) Measured results when spacing between two voltage multipliers is 5cm spacing and when spacing between two voltage multipliers is 10cm.

VII. SUGGESTED APPLICATIONS OF LATERAL-WAVE-BASED WPT IN AREAS OF WIRELESS COMMUNICATION

Many research efforts have been devoted to incorporating the technology of WPT into the existing communication devices, in which surface waves including the above-mentioned lateral waves are definitely applicable. Since space waves and surface waves differ not only in terms of transmission efficiency, but also in terms of mode of propagation, they can potentially be applied differently in the areas of wireless communication. In the following we introduce some conventional applications in the field of wireless communication where surface waves can be potentially useful. Also, an attempt to present potential applications in which surface waves might prove to be promising.

A. WIRELESS SENSOR NETWORK (WSNs)

In wireless sensor networks (WSNs), a set of sensor nodes are positioned in a specific area for collecting measurements of environmental parameters such as temperature, pressure, etc.

These measurements are then sent to a base station for further processing. A major limitation of WSNs is that the lifetime of sensors' batteries is short, and thus they need to be recharged periodically. To that end, the WPT technology is utilized by which a mobile charging vehicle is typically used to charge all sensor nodes wirelessly [24]. In particular, conventional radio-frequency based WPT technique such as inductive or resonance coupling is commonly used for that task; however, it suffers from the low-power efficiency due to the fact that, the harvested power scales inversely with the square of transmission distance, and also causes reduction in wireless throughput due to RF interferences as power RF signal is usually much stronger than the low-power data signal.

Since lateral waves can significantly increase the energy efficiency due to less signal attenuation compared with space waves, therefore, WPT based on lateral waves can be used for simultaneous charging of the sensor nodes more efficiently without causing harmful interference to wireless communications. In addition to inherent nature of lateral waves for interference reduction, the delivered power by lateral waves can also be conveyed on a lower frequency channel. In some scenarios where sensor nodes are deployed in partially or hardly accessible environment, RF based WPT becomes challenging. In such scenarios, the mobile charging vehicle may not be able to get close enough to sensor nodes or the existence of some physical obstacles renders power transfer highly inefficient or impossible. Thus, application of WPT based on lateral wave can be potentially very useful and promising, due to high-power transmission efficiency and the ability for complete interference avoidance.

B. SIMULTANEOUS WIRELESS INFORMATION AND POWER TRANSFER (SWIPT)

Another application of WPT is a scenario in which a source performs simultaneous transmission of wireless information and power to the destination nodes. However, there is always a tradeoff between harvested energy and delivered throughput, where many techniques in literature have been developed to achieve that. For instance, time switching and power splitting techniques, where data-power signal is split in time and power domains, respectively [25]. Undoubtedly, the strength of superimposed data-power signal is usually strong, which contributes to interference on other wireless communications as well as health risks. With a surface wave, however, these concerns can be totally eliminated.

Motivated by the technique of power line carrier communication (PLCC), both the power and the data signals for communication can be superimposed at different frequencies. As such, WPT based on lateral waves can be combined with frequency splitting technique in PLCC. It is possible to simultaneously transmit power and deliver data. The composite signal can be transmitted through the wall, the table top, the surface of ocean or the oxide layer coating any dielectric object in the form of multiple lateral waves in the absence of any radiation loss.

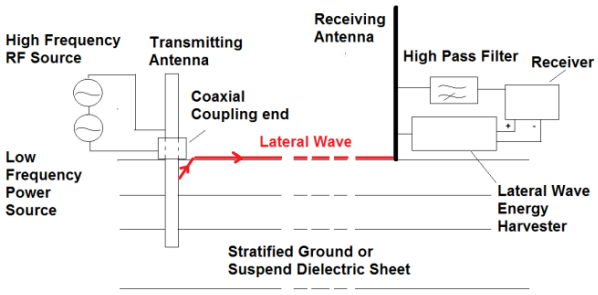

FIGURE 5. Example system integrating wireless communication and wireless power transfer together.

In practice, conventional monopole antennas can simultaneously handle more than one signals at different frequencies. The power can be preferably delivered at a lower frequency, say at any frequency below 500 MHz, where a highly concentrated lateral wave is easier to form. The signal to be transmitted can be a conventional WIFI signal or a signal at a much higher frequency. To ensure the delivered power does not impose any interference to the received signal, the energy to be processed by the receiver at the receiving end can be prefiltered with a high pass filter. Fig. 5 illustrates this scenario.

C. NLOS CHARGING OF A BLACK BOX FOR A DISAPPEARED FLIGHT

In the aftermath of the recent disappearance of passenger flight MH370 [26], the World Radiocommunication Conference (WRC-15) has reached an agreement to allocate the existing frequency band 1087.7-101092.3 MHz for passenger flights to the aeronautical mobile-satellite service (Earth-to-space) so that reception by space stations of Automatic Dependent Surveillance-Broadcast (ADS-B) emissions from the aircraft transmitters is possible. This extension obviously allows ADS-B signals to be transmitted beyond line-of-sight to facilitate reporting the position of missing aircraft equipped with ADS-B anywhere in the world. Whilst this extension will undoubtedly enhance the safety in skies, many disappeared flights failed to be tracked down after some months, mainly because of one reason; the black box or the flight data recorder (FDR) of the disappeared flight has simply run out of battery power.

FDR is an electronic device mounted in the rear part of almost all passenger flights. It records what happens inside the aircraft just before an air accident in order to facilitate a crash investigation. Inside the FDR, there is a device known as underwater locator beacon (ULB) which is supposed to be powered by a lithium battery and not normally switched on in the absence of any accident. Once the ULB becomes immersed into water, it is activated by a built-in ''water switch'' and sends out its ultrasonic 10ms pulse once per second at 37.5 kHz. These ultrasonic pulses are normally detectable 1–2 km away from water surface through space waves. In order for the ULB to operate as normal, the battery voltage must be in the range between 2.97 V and 3.5 V.

However, the battery power is sufficient for at most three months after the activation.

Incorporating a solar charger into the ULB design is one of the ways to maintain continuous operation of the ULB. In most air accidents, however, a disappeared flight usually ends up falling directly onto an area where natural light is not always available. Lateral waves together with trapped surface waves tend to follow the contour of the earth surface. It should come as no surprise that the FDR can also be equipped with a wireless energy harvester in much the same way as discussed in Section V. Theoretically, it is possible to remotely power or charge up the FDR of a misfortune aircraft through a lateral wave along the surface of the ocean bed or the ground, especially after the battery has run out. This feasibility will guarantee an uninterrupted tracking of ADS-B signal by the aeronautical mobile-satellite service.

If keeping the battery of an ULB/FDR alive becomes a reality, it should be equally possible in future to utilize so-called a lateral-wave radar to perform non-line-of-sight tracking of a disappeared flight or other hidden objects. What we need is to ground a highly directional monopole antenna with a beam scanning capability in the transmitting end.

VIII. DISCUSSIONS

The simulations and experimental results of this work can be straightforwardly concluded with two observations: a) the transmission efficiency of a wireless power can be significantly improved in the presence of a lateral wave; and b) the energy from lateral waves or space waves can be harvested by the proposed open-ended voltage multiplier. More importantly, the measured voltage is about 3 volts across the whole transmission range, suggesting that the proposed approach in this work can be used to wirelessly charge up a cell phones or other similar electronic appliances within 1 m away from the transmitting source.

The attenuation in configuration A obtained from our measurement as shown in Fig. 3c is 8.394 dB/m, whilst the simulated attenuation according to Fig. 4 is 8.82b dB/m. The simulation results roughly agree with the measurement in terms of attenuation although the shapes of both graphs are slightly different.

The measured voltage against distance for configuration A was found to be slightly sinusoidal over a long distance, whilst this effect is not obvious in the simulated magnetic field as shown in Fig. 4. This slight inconsistency is due to the fact that the model for space wave given in (6a) and (6b) was based on an assumption that the monopole antennas at the transmitting and receiving ends are electrically small. This assumption is not always valid, particularly for near field analysis.

On the other hand, both experimental and simulated results as shown in Figs 3c and 4 suggest that space waves alone are far too attenuated to support realistic transmission of wireless energy. Most of our simulation results suggest that the amplitude of the total magnetic field is lower than that of the lateral wave. In fact, space waves were found to be counterproductive in many of our WPT experiments.

Whilst the energy that can be harvested from a single observation point is limited, the experimental results as shown in Fig. 4b suggest that wireless energy can be harvested from more than one observation points as long as the spacing between two neighboring voltage multipliers are kept at half of the wavelength. This result suggests that the open-ended voltage multiplier can form a unit element of a rectanna array spanning an area so that more wireless energy can be harvested.

According to the results of our investigation, trapped surface waves are nowhere close to be a dominant propagation mode in far field. In almost all our experiments involving a thin dielectric layer in a stratified ground, the attenuation of a typical trapped surface wave was found to be substantially higher than that of the associated lateral wave. This is possibly because of the fact that trapped surface waves have to go through a much longer attenuated pathway than lateral waves. Lateral wave is guided by total internal reflection on the lower and upper interfaces of a dielectric layer, which is indeed a less attenuated pathway which bypasses free space. In addition, to support propagation of a trapped surface wave, the dielectric thickness should be greater than half of the wavelength. If a dielectric layer is excessively thin, however, trapped surface wave cannot by virtue exist but the intrinsic conductivity of dielectric layer will force the evanescent electromagnetic waves to propagate as a lateral wave in a highly confined volume, with a current density substantially higher than that of a space wave. There is no reason why one cannot take advantage of the lateral wave from stratified ground to improve the yield of a wirelessly harvested energy.

In contrast with the conclusions drawn by some other studies, the conductivity of this suspended dielectric layer does not have to be very high in order for a lateral wave to propagate efficiently along the air-dielectric interface.

Whilst free space is undoubtedly an acceptable medium for short range WPT, there remain many problems which cannot be solved by space waves alone. On the other hands, there remain many unexplored applications of lateral waves in the field of wireless communication. SWIPT and remote charging of a black box for a disappeared flight are just examples of those. The area of WPT based on lateral waves warrants more research for betterment of humanity.

IX. CONCLUSIONS

In this work, a model for the electromagnetic fields of a stratified ground with an imperfectly conducting bottom plane has been developed and used to simulate lateral waves propagating along the interface between air and a dielectric layer suspended in mid-air. The presence of a lateral wave has been experimentally verified in a configuration involving a thin table top. A wireless energy has been successfully harvested by direct voltage multiplication on a lateral wave, which has outperformed the space wave according to the prediction by the model. The device proposed for this direct voltage

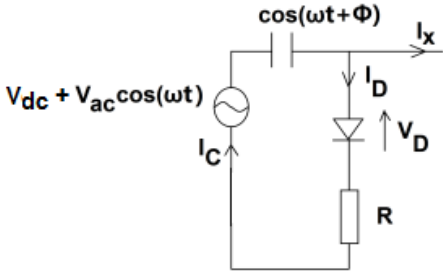

FIGURE 6. Circuit template for derivation of input/output relationship of the proposed open-ended voltage multiplier.

multiplication is an open-ended voltage multiplier with an open-circuited Goubau line to capture ambient electromagnetic field and with an output in the form of an enormously multiplied voltage. The simulated amplitude of the magnetic field at the receiving end was found to be inversely proportional to square root of the distance between the transmitter and the receiver. The simulation results were found to be in good agreement with the experimental outcome in terms of attenuation.

APPENDIX

Assume that we have a nonlinear circuit containing a voltage source, a diode, a capacitor and a load resistor connected in series as shown in Fig. 6. The voltage source contains a series cascade of a DC voltage V_{dc} and an AC voltage $V_{ac}cos(\omega t)$, where ω is the angular frequency in radian per second. The current in a diode is given as (A1):

$$I = I_s\left(\exp\left(\frac{V_D}{V_T}\right) - 1\right) \tag{A1}$$

where I_S is the reverse saturation current, V_T is the threshold voltage given by:

$$V_T = \frac{nKT}{q} \tag{A2}$$

n is the ideality factor and $KT/q = 26mV$ at room temperature. (A1) ignores the effect of the reverse breakdown voltage which can lead to an unpredictable decrease in the rectification efficiency of the proposed open-ended voltage multiplier.

(A1) can be rewritten according to the circuit information given in Fig. 6 as:

$$I_C = C\frac{dV_c\cos(\omega t+\phi)}{dt} = I_s\left(\exp\left(\frac{V_D}{V_T}\right)-1\right)+I_x \tag{A3}$$

where V_C and V_D are respectively the voltages across the capacitor and the diode in time domain. V_D in (2) can be substituted with $V_D = V_{dc} + V_{ac} - V_c - I_DR$, so that the following expression is obtained:

$$C\frac{dV\cos(\omega t+\phi)_c}{dt} = I_s\left(\exp\left(\frac{V_{dc}+V_{ac}\cos(\omega t)-V_c\cos(\omega t)-I_DR}{V_T}\right)-1\right)+I_x \tag{A4}$$

Integrating both sides of (A3) yields:

$$\frac{C}{\tau}\int_{V_c\cos(0+\varphi)}^{V_c\cos(\pi+\varphi)} \exp\left(\frac{V_c\cos(\omega t+\varphi)}{V_T}\right) dV_c\cos(\omega t+\varphi)$$
$$= \frac{1}{2\pi}\exp\left(\frac{V_{dc}-I_DR}{V_T}\right)\int_0^{\tau/2}\exp\left(\frac{V_{ac}\cos(\omega t)}{V_T}\right)d\omega t$$
$$-\frac{1}{2\pi}(I_s-I_x)\int_0^{\tau/2}\exp\left(\frac{V_c\cos(\omega t+\varphi)}{V_T}\right)d\omega t. \tag{A5}$$

Assuming the capacitance C is sufficiently large so that the AC voltage across the capacitance can be ignored, we can ignore the last term of (A4). The last term of (A4) involves I_x, which is the current leaking to other undisclosed parts of the circuit. This assumption means if the capacitance C is large enough, other parts of the circuit are NOT expected to affect the voltage of the diode to a significant extent.

The two integral terms on the right side of (A4) can be treated as modified Bessel integrals of the first kind. With this mind, and with the assumption on the value of C, expression in (A4) can be simplified into:

$$\frac{CV_T}{\tau}\exp\left(\frac{V_c\cos(\varphi)}{V_T}\right) \approx \exp\left(\frac{V_{dc}-I_DR}{V_T}\right)I_0\left[\frac{V_{ac}}{V_T}\right]. \tag{A6}$$

With some algebraic arrangement, the DC voltage across the capacitor as shown in Fig. 6 can be expressed:

$$V_c\cos(\varphi) \approx V_{dc} - I_DR + V_T\ln\left(\frac{1}{CfV_T}I_0\left[\frac{V_{ac}}{V_T}\right]\right). \tag{A7}$$

Therefore, the rectified voltage across diode can be expressed as:

$$V_D \approx -V_T\ln\left(I_0\left[\frac{V_{ac}}{V_T}\right]\right) + \ln(CfV_T) \tag{A8}$$

where $Io[\dots]$ is operator of the Bessel function of the first kind. In the schematic diagram as shown in Fig. 2a, the input of the circuit is a single-wire transmission line with a characteristic impedance anywhere between 200Ω and 550Ω. The electromagnetic energy in vicinity of the single-wire transmission line is captured into a transverse magnetic mode (TM mode) which is then rectified into a DC voltage by Avremenko's diode configuration formed by diodes *D1* and *D2*. However, the voltage across diodes *D1* and *D2* is not a pure DC voltage. They carry AC harmonics which are multiplied by the differential voltage multiplication process due to diodes *D3-D6* and capacitors C_1-C_4.

Capacitors C_1-C_4 serve as an AC short connected in a manner to make sure the AC voltage across each of the diodes *D1-D4* is maximized to approximately *2* $V_D(t)$. Since (A8) relates the rectified voltage to the AC source, we can use the same formula as a template to derive the rectified voltage across diodes *D3*, *D4*, *D5* and *D6* in terms of the AC voltages

across diodes *D1*and *D2*. Therefore, the voltage output of the circuit as shown in Fig. 2a can be expressed as:

$$V_{out} \approx +2V_D + 4V_T \ln\left(I_0\left[\frac{2V_D(t)}{V_T}\right]\right) - 4\ln\left(CfV_T\right). \tag{A9}$$

Equation (A9) can be approximated using the Bessel approximation formula into (A10):

$$V_{out} = 10V_D - \frac{nKT}{q}\ln\left[\frac{4\pi qV_D}{nKT}\right] + \frac{2nKT}{q}\ln\left[\frac{qI_S}{nCfnKT}\right]. \tag{A10}$$

REFERENCES

[1] G. Marconi, *Wireless Telegraphic Communication: Nobel Lecture, Dec. 11, 1909, Nobel Lectures, Physics 1901-1921*. Amsterdam, The Netherlands: Elsevier, 1967.

[2] G. Marconi, "The inventor of wireless telegraphy: A reply," *Saturday Rev.*, vol. 93, pp. 556–557, May 1902.

[3] S. P. Thompson, "Wireless telegraphy: A rejoinder," *Saturday Rev.*, vol. 93, pp. 598–599, May 1902.

[4] F. Carassa, "On the 80th anniversary of the first transatlantic radio signal," *IEEE Antennas Propag. Soc. Newslett.*, vol. 24, no. 6, pp. 10–19, Dec. 1982.

[5] G. Marconi, "Wireless telegraphy," *J. Inst. Elect. Eng.*, vol. 28, pp. 273–291, 1899.

[6] P. K. Bondyopadhyay, "Guglielmo Marconi—The father of long distance radio communication—An engineer's tribute," in *Proc. 25th Eur. Microw. Conf.*, Sep. 1995, pp. 879–885.

[7] P. Mazzinghi and G. Pelosi, "Enrico Fermi talks about Guglielmo Marconi [historical corner]," *IEEE Antennas Propag. Mag.*, vol. 53, no. 3, pp. 226–230, Jun. 2011.

[8] J. Zenneck, "Propagation of plane EM waves along a plane conducting surface," *Annal. Phys.*, vol. 28, pp. 846–866, Sep. 1907.

[9] A. Sommerfeld, "Propagation of waves in wireless telegraphy," *Annal. Phys.*, vol. 28, no. 3, pp. 665–736, 1909.

[10] A. N. Sommerfeld, "Propagation of waves in wireless telegraphy," *Annal. Phys.*, vol. 81, pp. 1135–1153, Dec. 1926.

[11] H. Weyl, "The propagation of electromagnetic waves over a plane conductor," *Annal. Phys.*, vol. 60, pp. 481–500, Nov. 1919.

[12] B. van der Pol and K. F. Niessen, "Über die Ausbreitung elektromagnetischer Wellen über eine ebene Erde," *Annal. Phys.*, vol. 398, no. 3, pp. 273–294, 1930.

[13] J. R. Wait, "The ancient and modern history of EM ground-wave propagation," *IEEE Antennas Propag. Mag.*, vol. 40, no. 5, pp. 7–24, Oct. 1998.

[14] J. D. Cross and P. R. Atkins, "Electromagnetic propagation in four-layered media due to a vertical electric dipole: A clarification," *IEEE Trans. Antennas Propag.*, vol. 63, no. 2, pp. 870–886, Feb. 2015.

[15] R. W. P. King, M. Owens, and T. T. Wu, *Lateral Electromagnetic Waves*. Berlin, Germany: Springer-Verlag, 1992.

[16] T. Tamir, "Experimental verification of a lateral wave above a lossy interface," *Electron. Lett.*, vol. 6, no. 12, pp. 357–358, Jun. 1970.

[17] T. Tamir and D. Staiman, "Nature and optimisation of the ground (lateral) wave excited by submerged antennas," *Proc. IEEE*, vol. 113, no. 8, pp. 1299–1310, Aug. 1986.

[18] N. Tesla, *The True Wireless* (Electrical Experimenter). USA: Electrical Experimenter, May 1919.

[19] D. Stration, S. Lange, and J. M. Inal, "Pulsed extremely low-frequency magnetic fields stimulate microvesicle release from human monocytic leukaemia cells," *Biochem. Biophys. Res. Commun.*, vol. 430, no. 2, pp. 470–475, Jan. 2013.

[20] K. Li, *Electromagnetic Fields in Stratified Media*. Hangzhou, China: Zhejiang Univ. Press, 2009.

[21] L. W. Liu, A. Kandwal, Z. E. Eremenko, and Q. Zhang, "Open-ended voltage multipliers for wireless transmission of electric power," *J. Microw. Power Electromagn. Energy*, vol. 25, no. 3, pp. 187–204, Aug. 2017.

[22] N. E. Zaev, S. V. Avramenko, and V. N. Lisin, "Messen des Leitungsstroms, die Polarisation des erregten Strom," *Russian J. Phys. Gedanken*, no. 2, 1991.

[23] L. W. Y. Liu, S. Ge, Q. Zhang, and Y. Chen, "Capturing surface electromagnetic energy into a DC through single-conductor transmission line at microwave frequencies," *Prog. Electromagn. Res. M*, vol. 54, pp. 29–36, Jan. 2017.

[24] L. Xie, Y. Shi, Y. T. Hou, and A. Lou, "Wireless power transfer and applications to sensor networks," *IEEE Wireless Commun.*, vol. 20, no. 4, pp. 140–145, Aug. 2013.

[25] R. Zhang and C. K. Ho, "MIMO broadcasting for simultaneous wireless information and power transfer," *IEEE Trans. Wireless Commun.*, vol. 12, no. 5, pp. 1989–2001, May 2013.

[26] M. A. Mujeebu, "The disappearance of MH370 and the search operations—The role of technology and emerging research challenges," *IEEE Aerosp. Electron. Syst. Mag.*, vol. 31, no. 3, pp. 6–16, Mar. 2016.

[27] N. Tesla, "The transmission of electrical energy without wires as a means for furthering peace," *Elect. World Eng.*, pp. 21–24, Jan. 1905.

[28] R. W. P. King and S. S. Sandler, "The electromagnetic field of a vertical electric dipole in the presence of a three-layered region," *Radio Sci.*, vol. 29, pp. 97–113, Jan./Feb. 1994.

[29] R. E. Collin, "Some observations about the near zone electric field of a hertzian dipole above a lossy earth," *IEEE Trans. Antennas Propag.*, vol. 52, no. 11, pp. 3133–3137, Nov. 2004.

[30] R. E. Collin, "Hertzian dipole radiating over a lossy earth or sea: Some early and late 20th-century controversies," *IEEE Antennas Propag. Mag.*, vol. 46, no. 2, pp. 64–79, Apr. 2004.

[31] L. W. Y. Liu, Q. Zhang, and Y. Chen, "Harvesting atmospheric ions using surface electromagnetic wave technologies," *J. Adv. Technol. Innov.*, vol. 2, no. 4, pp. 99–104, 2017.

[32] G. Lodovico. (Jun. 26, 2000). *Marconi and the Overthrow of the Historical Truth About his Work*. [Online]. Available: http://www.radiomarconi.com/

[33] P. K. Bondyopadhyay, "Sir JC Bose's diode detector received Marconi's first transatlantic wireless signal of December 1901 (The 'Italian Navy Coherer' Scandal Revisited)," *Proc. IEEE*, vol. 86, no. 1, pp. 259–285, Jan. 1998.

[34] N. Tesla, "On light and other high frequency phenomena," *J. Franklin Inst.*, vol. 136, pp. 1–19, Jul. 1893.

[35] N. Tesla, "On light and other high frequency phenomena," *J. Franklin Inst.*, vol. 136, no. 4, pp. 259–279, Oct. 1893.

[36] N. Tesla, "High frequency oscillators for electro-therapeutic and other applications," *Elect. Eng.*, vol. 26, no. 550, pp. 1282–1292, Nov. 1898.

LOUIS WY LIU received the degree (Hons.) in electrical and electronics engineering from Sunderland University, U.K., in 1989, received the Ph.D. degree from the Institute of Microwave and Photonics, University of Leeds, U.K., in 2001. During his Ph.D. degree, he was a Researcher Engineer with the Momentum Team, Agilent Technologies, Gent, Belgium. He was a Post-Doctoral Research Fellow with the Radiation Laboratory, Michigan University, Ann Arbor, USA, from 2001 to 2003. He is currently with the Southern University of Science and Technology, China. His current research interests include wireless power transfer, energy harvesting from microwave and ultra-violet rays, trapped surface waves, single-wire power transfer, antenna design, surface plasmon polariton, terahertz engineering, microneedles, and 3-D micro-/nano-fabrication.

QINGFENG ZHANG received the B.E. degree in electrical engineering from the University of Science and Technology of China, Hefei, China, in 2007, and the Ph.D. degree in electrical engineering from Nanyang Technological University, Singapore, in 2011. From 2011 to 2013, he was with the Poly-Grames Research Center, Ecole Polytechnique de Montreal, Montreal, Canada, as a Post-Doctoral Fellow. Since 2013, he has been with the Southern University of Science and Technology, Shenzhen, China as an Assistant Professor. His research interests are focused on emerging novel electromagnetics technologies and multidisplinary topics.

YIFAN CHEN received the B.Eng. (Hons.) and Ph.D. degrees in electrical and electronic engineering from Nanyang Technological University in 2002 and 2006, respectively. From 2005 to 2007, he was a Project Officer and then a Research Fellow with the Singapore-University of Washington Alliance in bioengineering, supported by the Singapore Agency for Science, Technology and Research, Nanyang Technological University, Singapore, and the University of Washington at Seattle, USA. From 2007 to 2012, he was a Lecturer and then a Senior Lecturer with the University of Greenwich and Newcastle University, U.K. From 2012 to 2016, he was a Professor and the Head of Department of Electrical and Electronic Engineering, Southern University of Science and Technology, Shenzhen, China, appointed through the Recruitment Program of Global Experts—the Thousand Talents Plan. In 2013, he was a Visiting Professor with the Singapore University of Technology and Design, Singapore. He is currently with the University of Waikato, Hamilton, New Zealand, as a Professor of Engineering and the Associate Dean External Engagement of the Faculty of Science and Engineering and the Faculty of Computing and Mathematical Sciences, University of Waikato, Hamilton, New Zealand.

MOHAMMED A. TEETI received the Ph.D. degree in electrical engineering from the Huazhong University of Science and Technology, Wuhan, China, in 2015. He is currently a Post-Doctoral Fellow with the Department of Electronic and Electrical Engineering, Southern University of Science and Technology, Shenzhen, China. His current research interests are in the fields of wireless communications and information theory, with focus on massive MIMO, mmWave massive MIMO, and interference channels.

RANJAN DAS received B.E. degree in electronics and instrumentation engineering from Jadavpur University, and the master's degree with specialization in electronics systems design from the Electrical Engineering Department, IIT Bombay, where he currently pursuing the Ph.D. degree. He joined the Electronics and Electrical Engineering Department, South University of Science and Technology of China, Shenzhen, China, as a Visiting Student. His research area includes reconfigurable multiband filter design, synthesis of negative group delay circuits. He is also interested in real time analog signal processing for microwave frequencies.